Supporting Information for Rosell et al.(2023 -TEKTONIKA)

Holocene Earthquakes on the Tambomachay Fault near Cusco, Central Andes

Lorena Rosell[1*], Carlos Benavente[1,2], Swann Zerathe[1,3], Sam Wimpenny[4], Enoch Aguirre[1], Richard Walker[5], Christoph Grützner[6], Briant García[1], Laurence Audin[3], Andy Combey[3], Anderson Palomino[1], Fabrizio Delgado[2], Miguel Rodríguez-Pascua[7], José Cardenas[8], and Julien Carcaillet[3]

Corresponding author: *Lorena Rosell (*lrosell@ingemmet.gob.pe*)

[1] Instituto Geológico, Minero y Metalúrgico (INGEMMET), San Borja, Perú

[2] Especialidad Ingeniería Geológica, Facultad de Ciencias e Ingeniería. Pontificia Universidad Católica del Perú

[3] Univ. Grenoble Alpes, Univ. Savoie Mont Blanc, CNRS, IRD, IFSTTAR, ISTerre, 38000 Grenoble, France

[4] COMET, School of Earth and Environment, University of Leeds, Leeds, UK.

[5] COMET, Dept. of Earth Sciences, Oxford University, South Parks Road, Oxford OX1 3AN, UK

[6] Friedrich Schiller University Jena, Institute of Geological Sciences, Burgweg, 11 07749 Jena, Germany

[7] Instituto Geológico y Minero de España (IGME, CSIC). Ríos Rosas Street 23, 28022-Madrid, Spain

[8] Universidad Nacional de San Antonio Abad del Cusco (UNSAAC)

Table SI-1: Summary of locations and measured vertical offset and throw. See location on Figure S1.

Profile number	Sector	Longitude (°)	Latitude (°)	Offset (m)	Error (m)	Throw (m)	Error (m)	Litology	Source
1	Sencca Sector	-72.017600	-13.473970	4.2	0.3	4.8	0.9	Holocene fluvio-glacial deposit	Drone DEM (0.2m/px)
2		-72.016550	-13.473930	3.0	0.4	3.9	1.7	Holocene fluvio-glacial deposit	
3		-72.013170	-13.473370	2.3	0.6	3.0	1.6	Holocene fluvio-glacial deposit	
4		-72.012820	-13.473380	3.6	0.5	4.8	1.6	Holocene fluvio-glacial deposit	
5		-72.012450	-13.473390	2.2	0.6	3.0	1.8	Holocene fluvio-glacial deposit	
6		-72.012020	-13.473430	4.3	0.4	4.9	1.0	Holocene fluvio-glacial deposit	
7		-72.011360	-13.473610	8.4	0.3	9.0	0.7	Holocene fluvio-glacial deposit	
8		-72.011030	-13.472840	2.5	0.3	2.8	0.6	Holocene fluvio-glacial deposit	
9		-72.010380	-13.473140	3.5	0.2	4.1	0.8	Holocene fluvio-glacial deposit	
10		-72.008710	-13.471760	3.9	0.5	5.0	1.7	Bedrock	
11		-72.006410	-13.473590	3.4	0.6	3.6	1.4	Holocene fluvio-glacial deposit	
12	Pumamarca Sector	-71.990960	-13.470490	13.4	1.3	17.2	4.5	Bedrock	Pleiades DEM (1.53m/px)
13		-71.976210	-13.472450	2.5	0.6	3.1	1.5	Quaternary alluvial deposits	
14		-71.974340	-13.473630	5.4	0.7	8.5	6.3	Bedrock	
15		-71.971770	-13.474260	6.4	0.8	8.2	2.6	Bedrock	
16		-71.970470	-13.474810	4.5	0.6	5.4	1.4	Quaternary alluvial deposits	
17		-71.964680	-13.476400	3.3	0.5	4.5	2.0	Bedrock	
18		-71.962930	-13.477000	5.6	0.9	7.2	2.5	Bedrock	
19		-71.957630	-13.479230	7.7	0.8	9.3	2.4	Bedrock	
20		-71.946910	-13.484460	9.1	0.9	10.8	2.6	Bedrock	
21		-71.945640	-13.484510	4.9	0.6	6.4	2.3	Bedrock	

Table SI-2: Cosmogenic nuclide data (^{10}Be). Z is the sample thickness, S is the topographic shielding factor. All the uncertainties reported are 1 sigma. Exposure ages are calculated with the CREp program (Martin et al., 2017) considering zero erosion.

Sample	Latitude (S°)	Longitude (W°)	Elevation (m a.s.l.)	Z (cm)	S (%)	Mass (g)	^{9}Be carrier (10^{19} atoms)	^{10}Be/^{9}Be (10^{-14})	^{10}Be [a] (10^{5} at.g^{-1})	Exposure ages [b] (ka)
T1	13.472728	72.010258	4180	2.5	0.989	6.747	3.17	9.79 ± 0.28	4.53 ± 0.15	14.2 ± 0.4 (0.5)
T2	13.473045	72.010327	4181	3.5	0.989	3.362	3.25	4.93 ± 0.18	4.62 ± 0.30	14.5 ± 0.8 (0.9)
T3	13.473272	72.010371	4174	3.5	0.987	4.271	3.26	6.58 ± 0.27	4.92 ± 0.22	15.3 ± 0.5 (0.7)
T4	13.473653	72.010560	4168	5.0	0.993	6.244	3.11	8.25 ± 0.27	4.03 ± 0.15	13.0 ± 0.5 (0.6)
T5	13.473300	72.012022	4167	3.5	0.979	6.946	3.11	9.77 ± 0.29	4.31 ± 0.14	13.9 ± 0.4 (0.6)
T6	13.473842	72.011988	4152	5.0	0.993	10.012	3.25	14.25 ± 0.37	4.58 ± 0.13	14.7 ± 0.3 (0.5)
T7	13.474122	72.011994	4144	5.5	0.993	11.637	3.09	17.36 ± 0.45	4.57 ± 0.14	14.7 ± 0.4 (0.5)
T8	13.474206	72.016800	4135	5.5	0.969	5.621	3.15	7.61 ± 0.27	4.18 ± 0.17	14.0 ± 0.5 (0.6)
T9	13.474517	72.017120	4124	5.5	0.969	13.825	3.21	19.76 ± 0.45	4.56 ± 0.12	15.1 ± 0.3 (0.5)
T10A	13.474063	72.018399	4123	4.0	0.968	11.881	3.21	16.17 ± 0.40	4.33 ± 0.12	14.4 ± 0.3 (0.5)

T10B	13.474063	72.018399	4123	3.5	0.968	11.089	3.21	14.82 ± 0.37	4.25 ± 0.12	14.1 ± 0.4 (0.5)
T11	13.474433	72.018440	4110	4.5	0.961	3.847	3.21	5.8 ± 0.23	4.71 ± 0.20	15.6 ± 0.5 (0.7)

[a] Uncertainties reported include the counting statistics, the machine stability (~0.5%) and the blank correction which has a $^{10}Be/^{9}Be$ ratio of 1.58 ± 0.59 x 10^{-15} for this run.

[b] Exposure ages are reported with analytical and total uncertainties (the total uncertainty is in parentheses), that both include the propagation of uncertainties of each parameter by partial derivatives such as described in Marrero et al. (2016). Production rate: weighted mean of Kelly et al. (2015) and Martin et al. (2015) - Scaling: Lal-Stone modified - Atmosphere: ERA40 - VDM: Muscheler et al. (2005).

Table SI-3: Exposure ages calculated considering an erosion rate of $5*10^{-4}$ cm.a^{-1} (value estimated by Kelly et al., 2015). Dataset analyzed with P-CAAT (Dortch et al., 2022) using the Std/IQR bandwidth estimator (bandwidth = 0.3780 ka; r-sq = 0.9999) give a highest probability gaussian distribution with a peak at 14.90 ± 0.49 ka.

Sample	Exposure ages (ka)
T1	14.9 ± 0.4 (0.5)
T2	15.2 ± 0.8 (0.9)
T3	16.1 ± 0.6 (0.7)
T4	13.7 ± 0.5 (0.6)
T5	14.5 ± 0.4 (0.5)
T6	15.4 ± 0.4 (0.5)
T7	15.5 ± 0.4 (0.5)
T8	14.7 ± 0.5 (0.6)
T9	15.9 ± 0.3 (0.5)
T10A	15.1 ± 0.3 (0.5)
T10B	14.8 ± 0.3 (0.5)
T11	16.4 ± 0.6 (0.7)

Table SI-4: Summary table of the ^{14}C modeled ages from the Tambomachay trench

No	Sample code	Beta code	Stratigraphic unit	Dated material	d13C (o/oo)	Uncalibrated age * (BP)	Unmodelled calibrated age * (BP)	Unmodelled σ	Modelled calibrated age (BP)	Modelled σ
1			U7						1074-538	140
2	GA-50-045	Beta-460594	C3 (top)	Organic sediment	-25.6	1190 +/- 30 BP	1178-960	55	1095-957	40
3			C3 (base)						1190-974	58
4			Surface rupture event 3						1259-1034	61
5	GA-50-044	Beta-460593	U6 (top)	Organic sediment	-25.7	1310 +/- 30 BP	1275-1080	55	1281-1111	41
6			U6 (base)						3353-1179	749
7	GA-50-037	Beta-460586	U5 (near to the top)	Organic sediment	-25.6	3120 +/- 30 BP	3377-3178	51	3358-3176	46
8	GA-50-036	Beta-460585	U5 (near to the base)	Organic sediment	-25.9	3140 +/- 30 BP	2291-3212	50	3392-3244	41
9			U5(base)						4595-3260	421
10	GA-50-043	Beta-460592	C2 (top)	Organic sediment	-25.3	4140 +/- 30 BP	4818-4448	97	4819-4449	97
11	GA-50-038	Beta-460587	C2 (base)	Organic sediment	-25.4	4870 +/- 30 BP	5650-5475	50	5650-5473	50
12			Surface rupture event 2						6716-5585	350
13	GA-50-039	Beta-460588	U4 (near to the top)	Organic sediment	-25.4	5890 +/- 30 BP	6782-6556	55	6780-6555	55
14			U4 (base)						7125-6640	132
15	GA-50-040	Beta-460589	U3 (near to the top)	Organic sediment	-25.6 o/oo	6190 +/- 30 BP	7163-6943	67	7163-6944	67
16			U3 (base)						8175-6959	345
17			U2						8450-7590	245
18	GA-50-041	Beta-460590	C1	Organic sediment	-25.1 o/oo	7640 +/- 30 BP	8515-8344	32	8442-8352	22
19	GA-50-046	Beta-460595	C1	Organic sediment	-25.5 o/oo	7680 +/- 30 BP	8536-8378	43	8520-8383	36
20			C1 (base)						9333-8377	369
21			Surface rupture event 1						12371-8401	1279
22			U1						14662-8466	1848

Figure SI-1: Workflow used for calculating the fault throw from a fault scarp. (a) 3D hillshade from Pleaides DEM showing the moraines, the fault segments and location of profiles in the Sencca sector (see Table S1). (b) 3D analysis of the aspect of the hangingwall and footwall surfaces. (c) Two-dimensional analysis for calculating the fault offset between the hangingwall and footwall surfaces at the point approximately in the center of the scarp. (d) Analysis of the dip of both surfaces. (e) Calculation of the fault throw from the fault offset in (b) and the slope geometry in (c,d) using the method of Mackenzie and Elliott (2017).

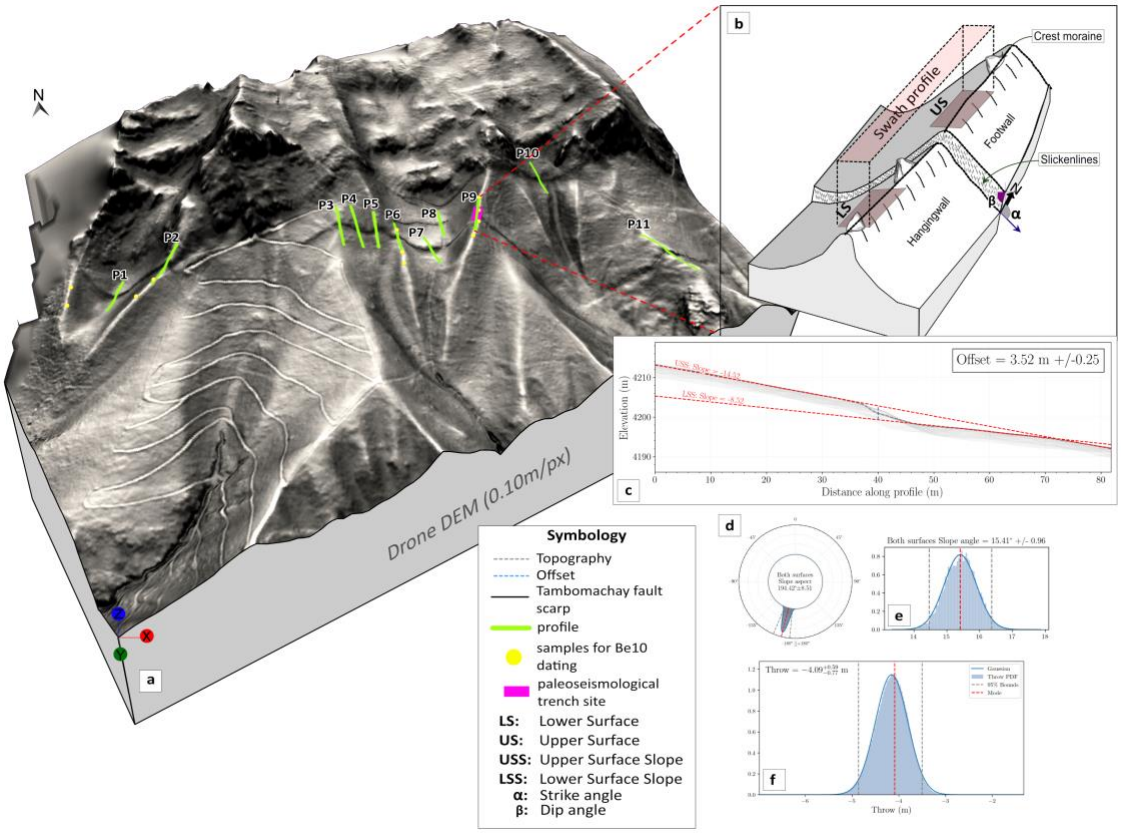

Figure SI-2: Detailed profiles from the Sencca and the Pumamarca sectors.

Profile 1

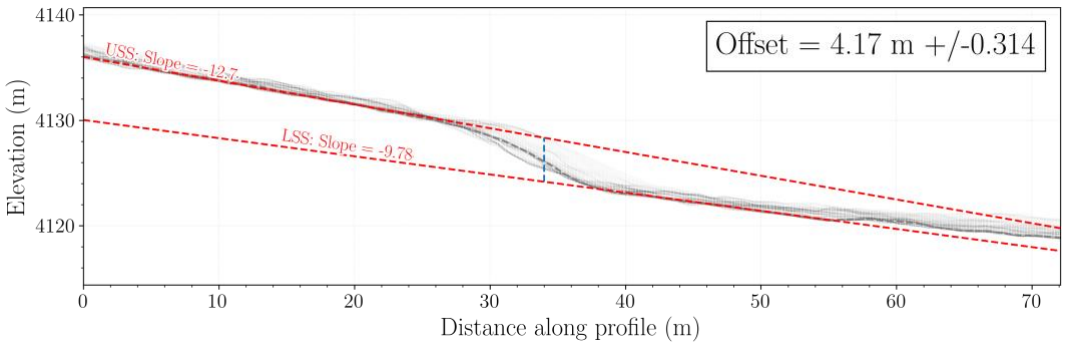

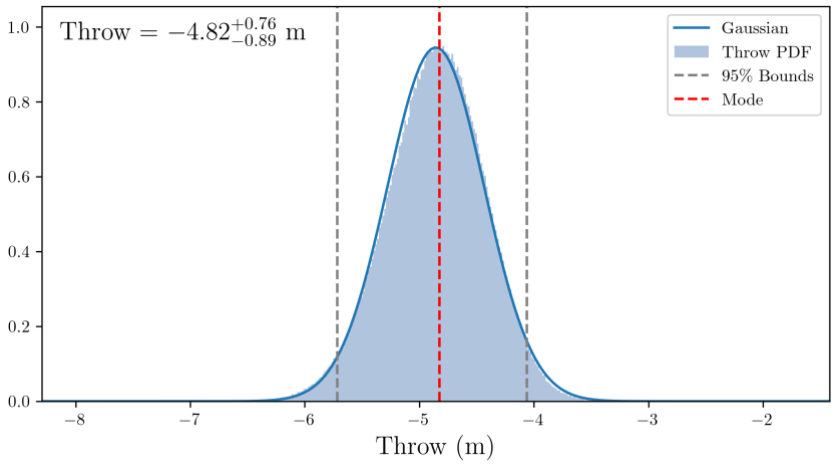

Profile 2

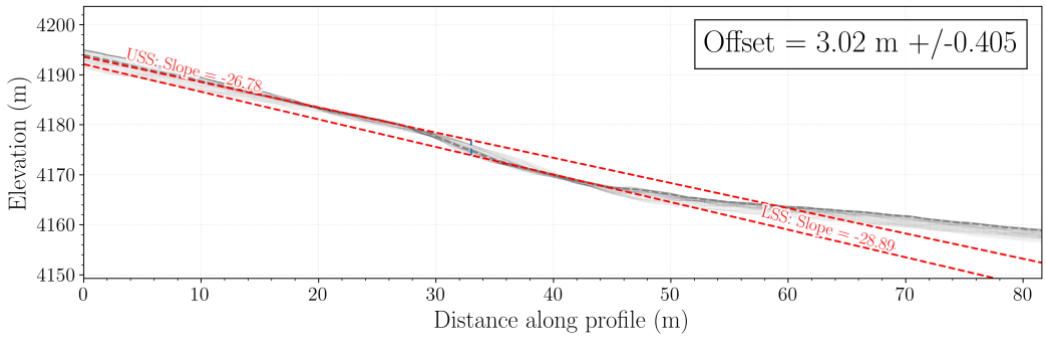

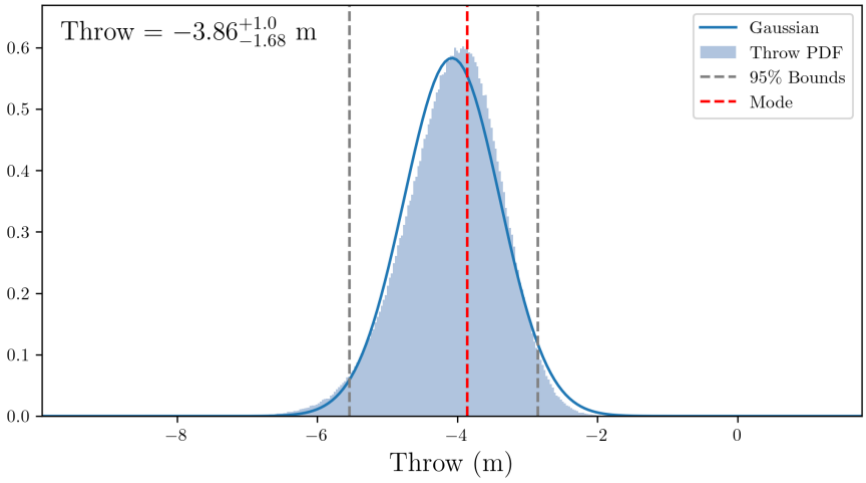

Profile 3

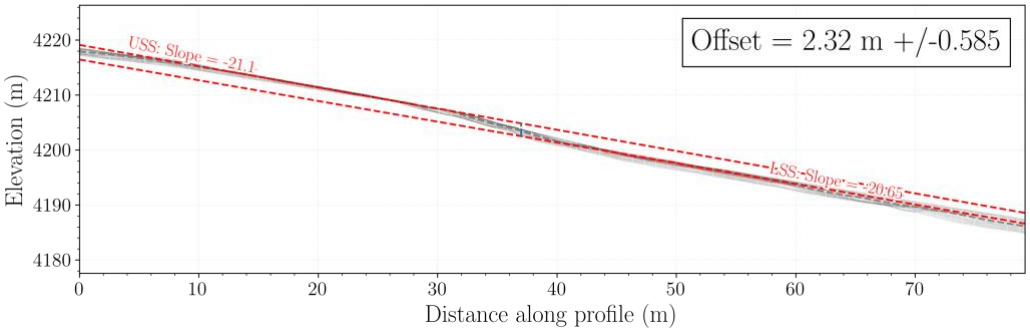

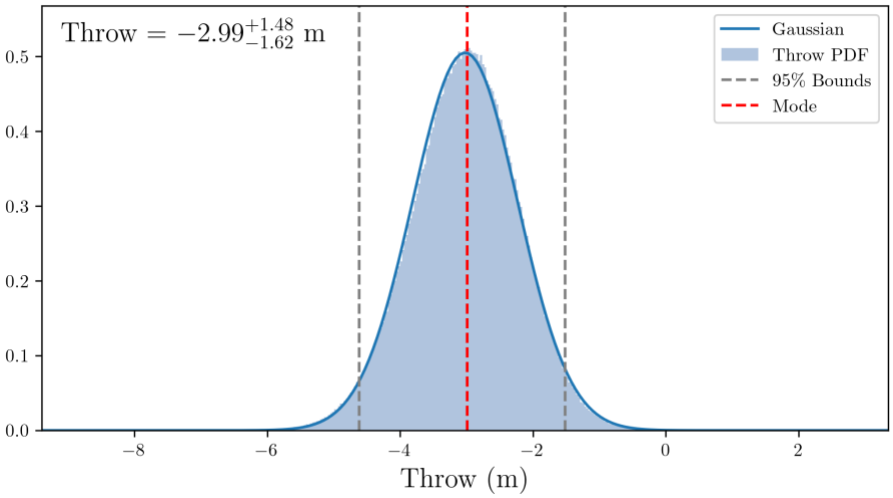

Profile 4

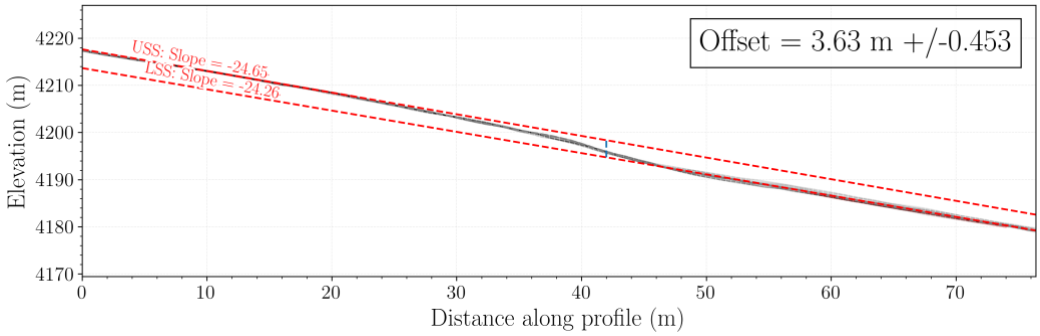

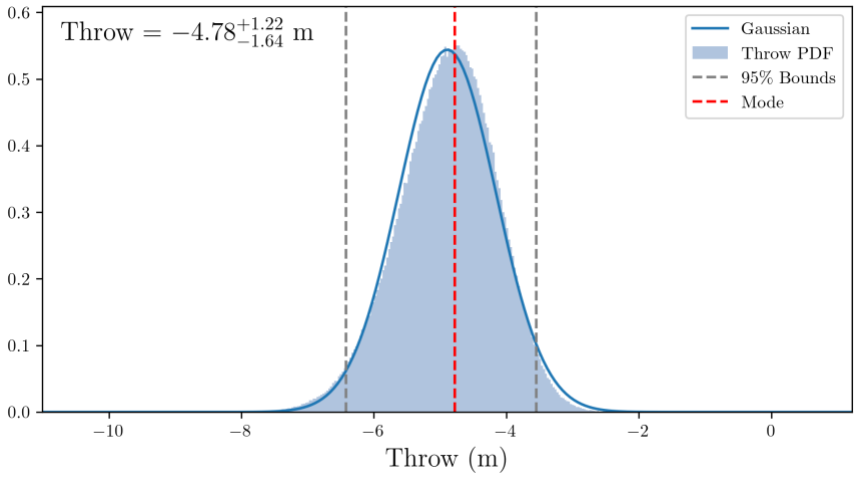

Profile 5

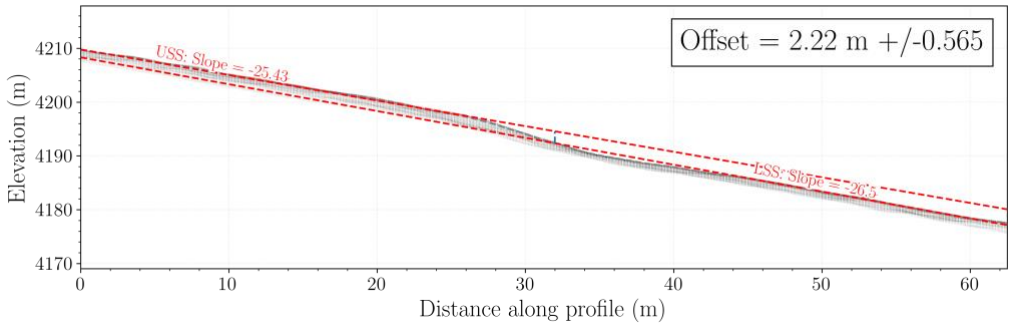

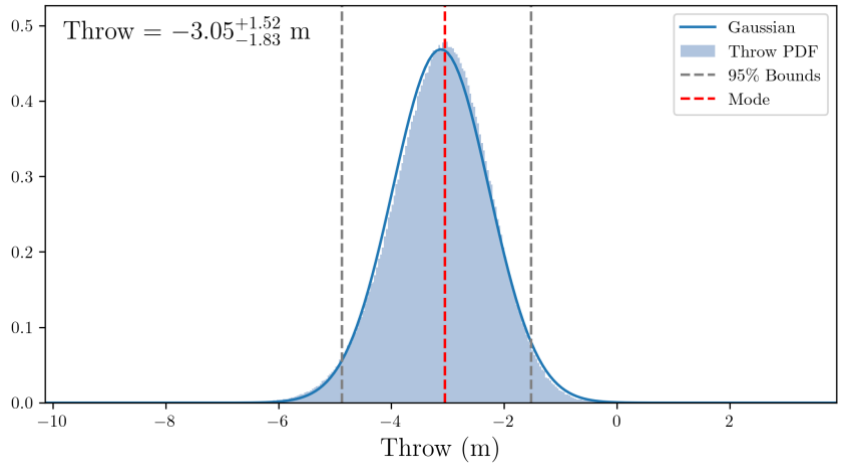

Profile 6

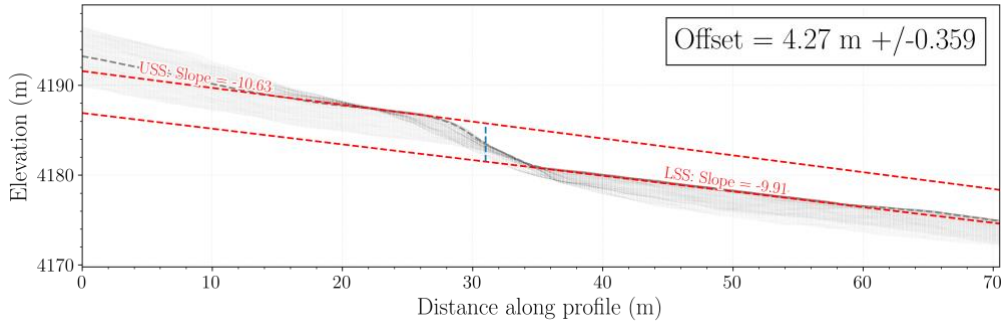

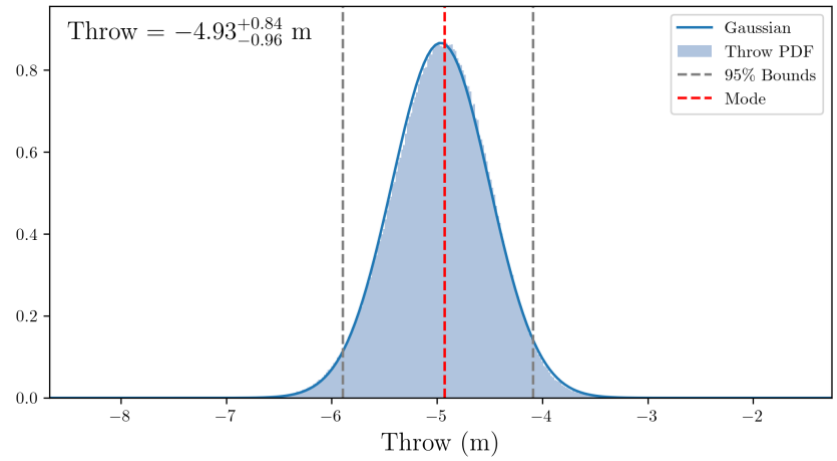

Profile 7

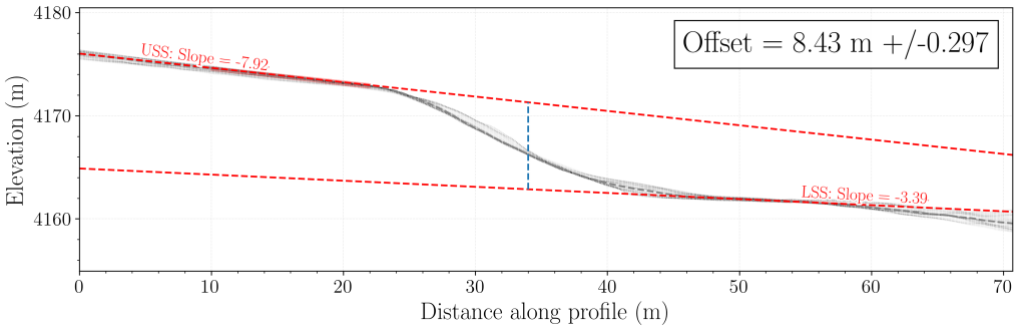

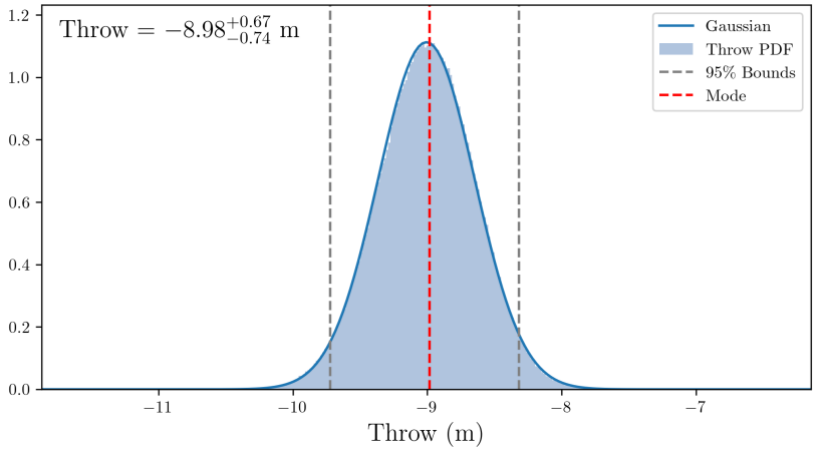

Profile 8

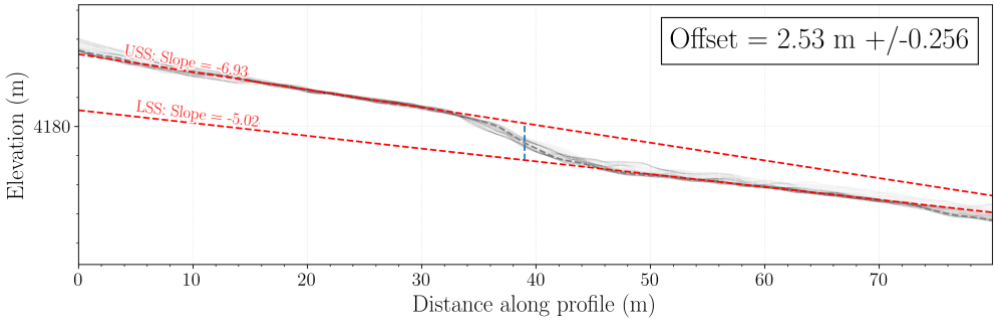

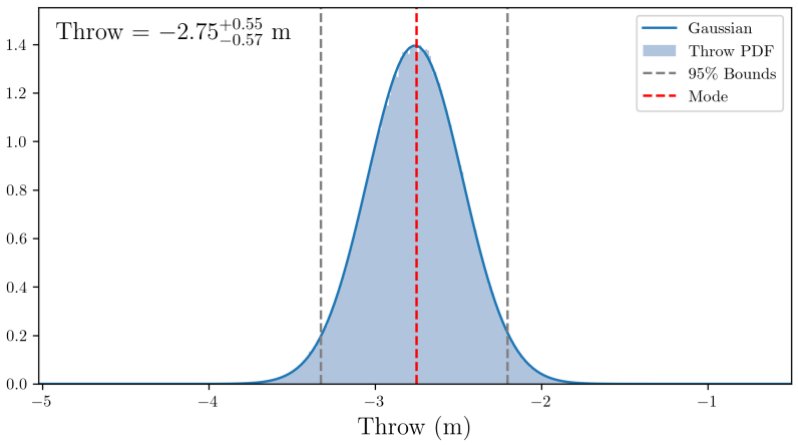

Profile 9

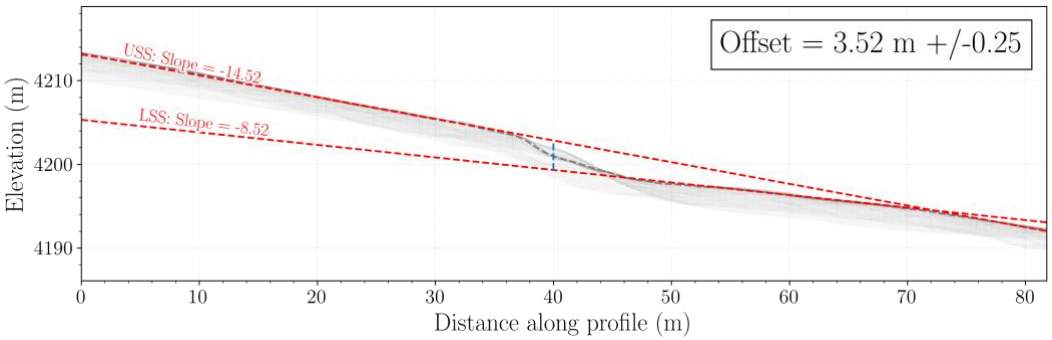

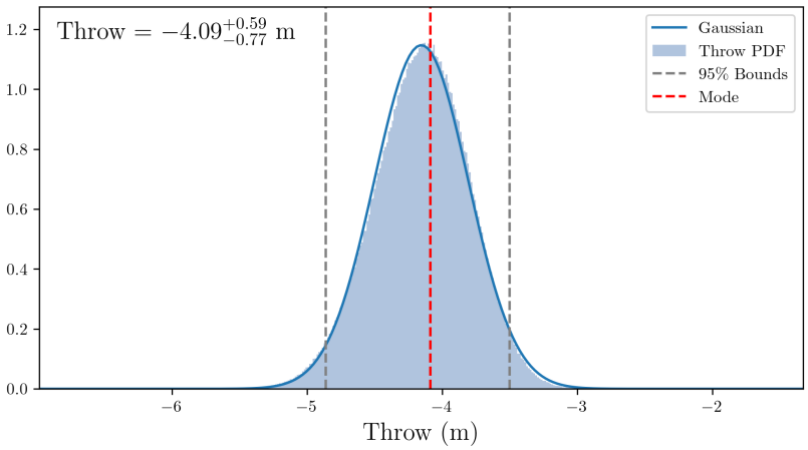

Profile 10

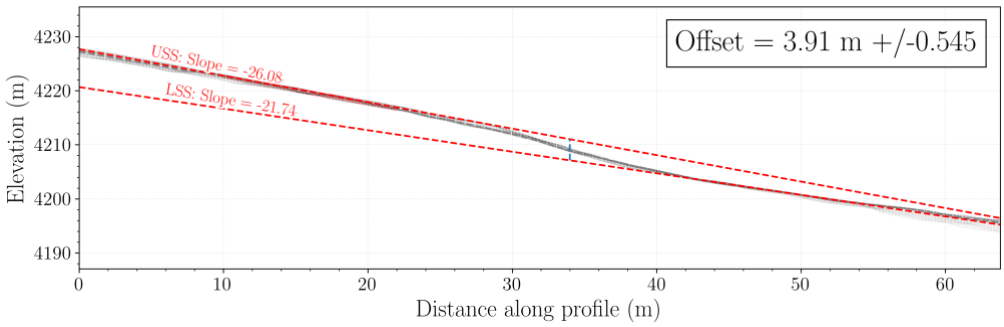

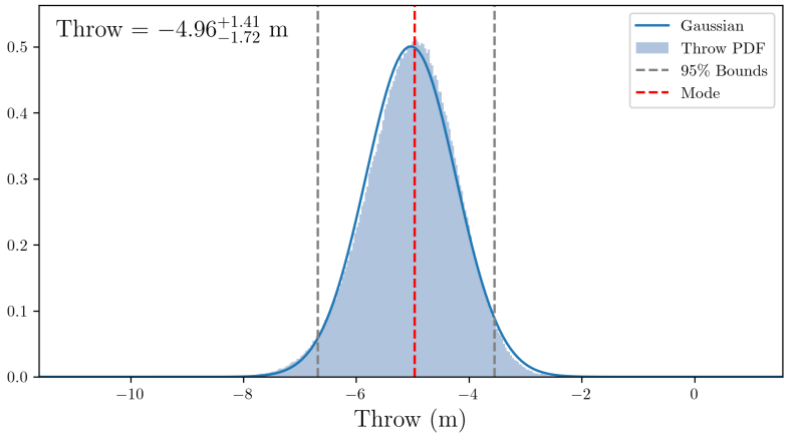

Profile 11

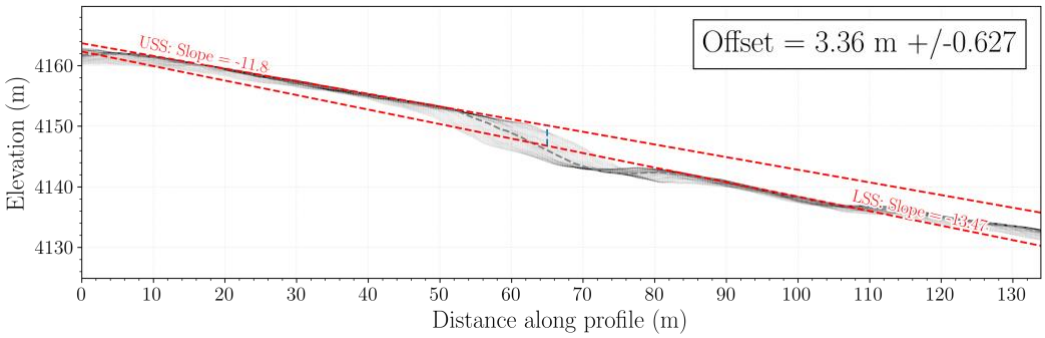

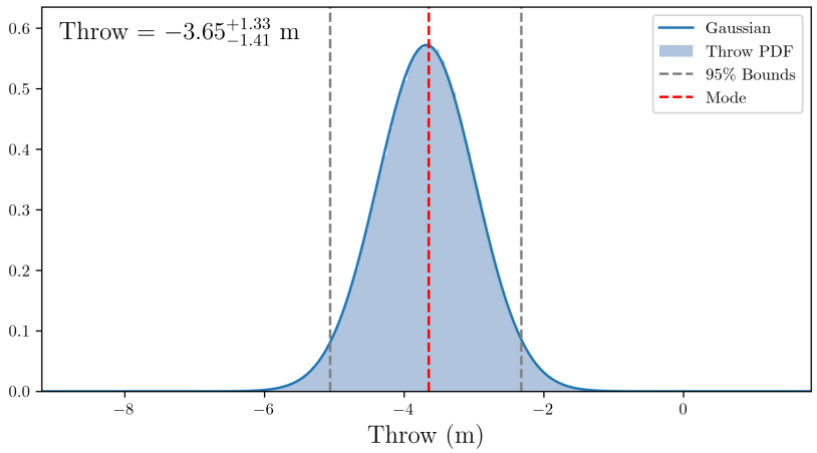

Profile 12

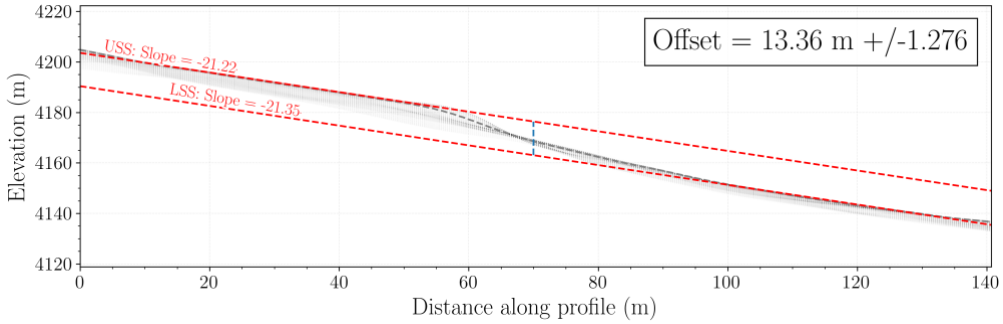

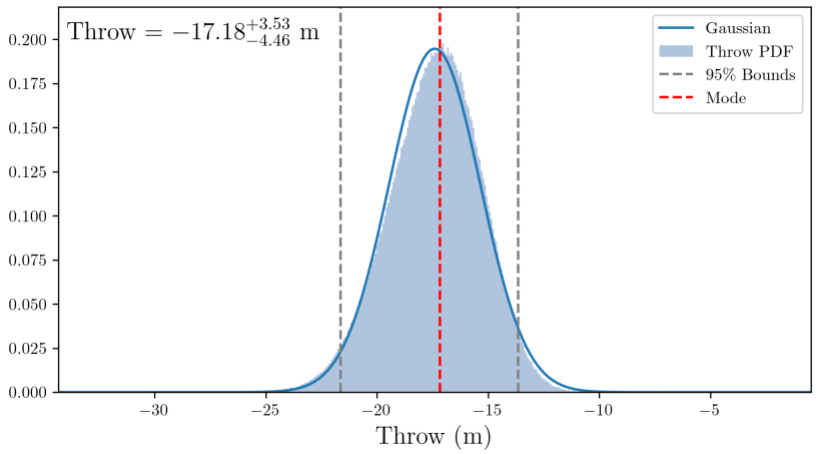

Profile 13

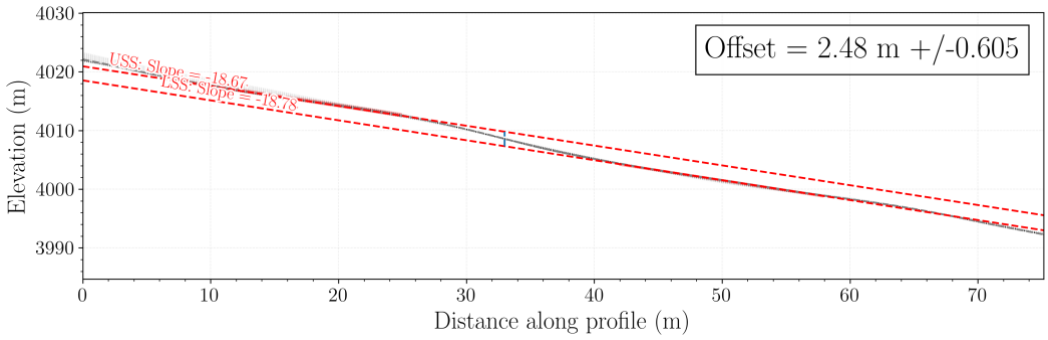

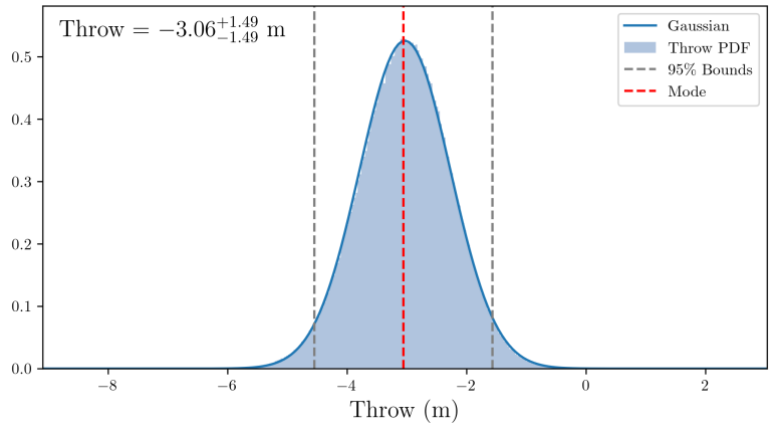

Profile 14

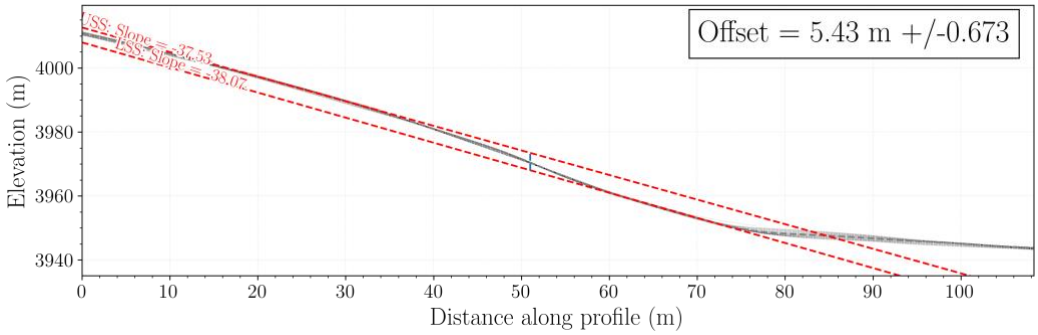

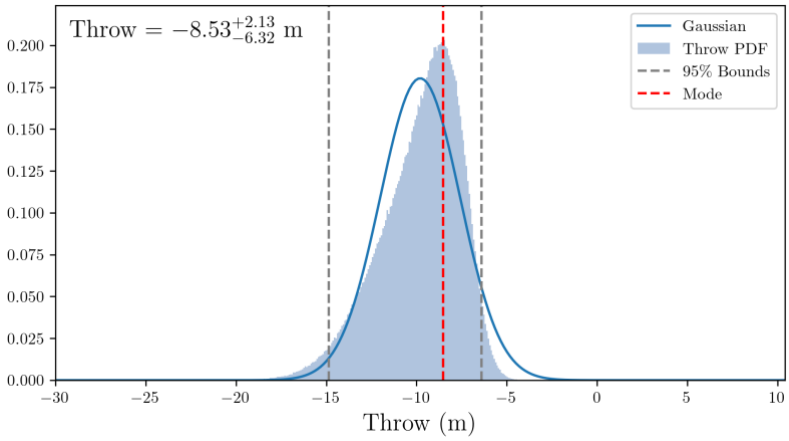

Profile 15

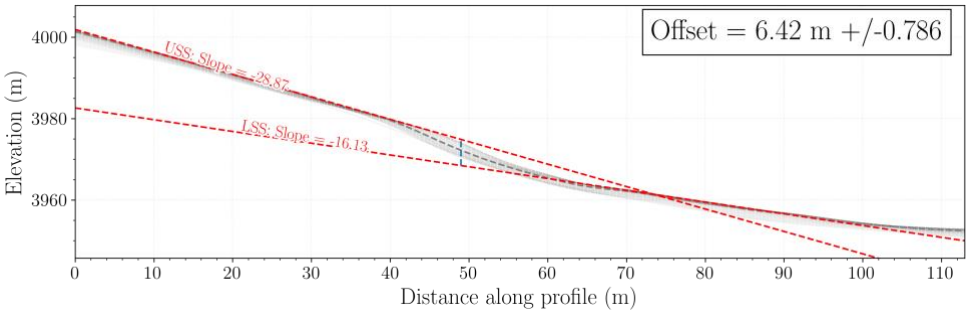

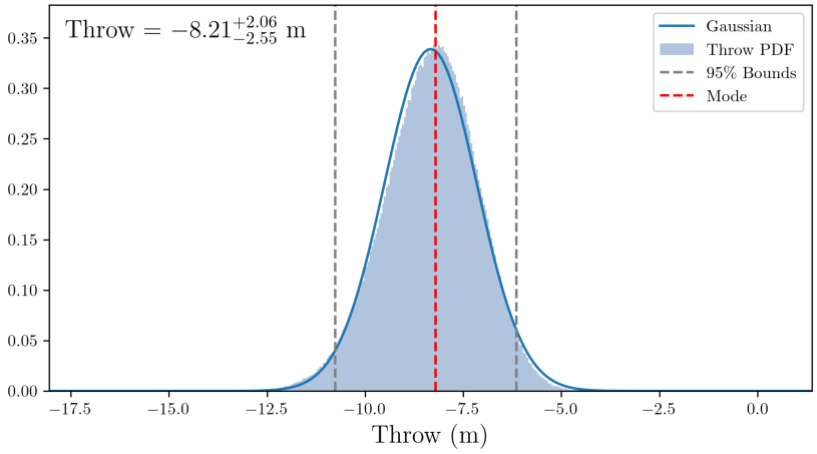

Profile16

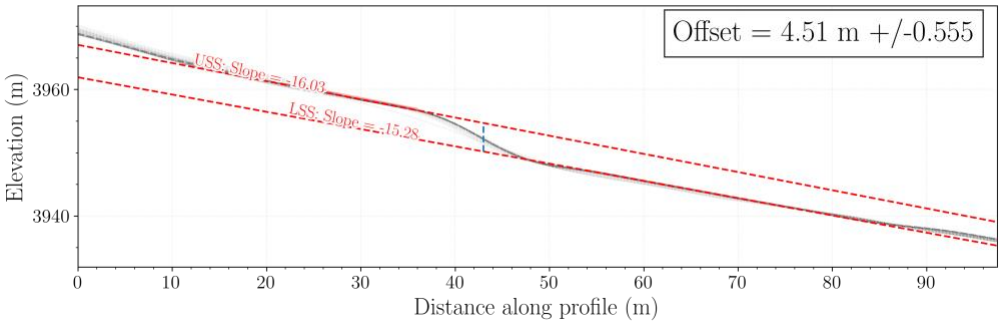

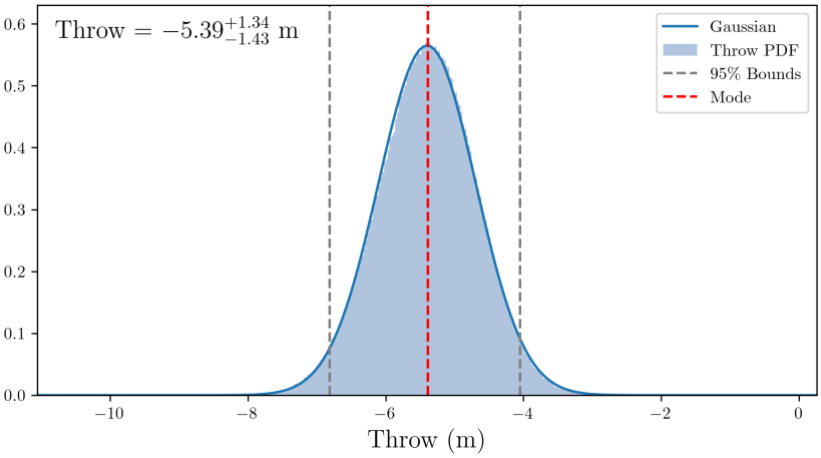

Profile 17

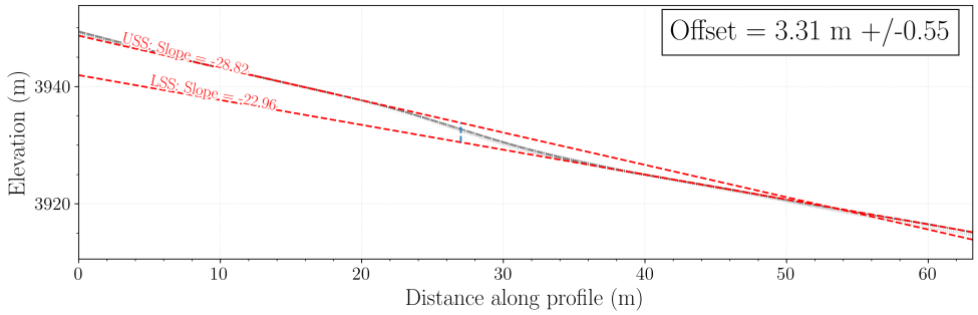

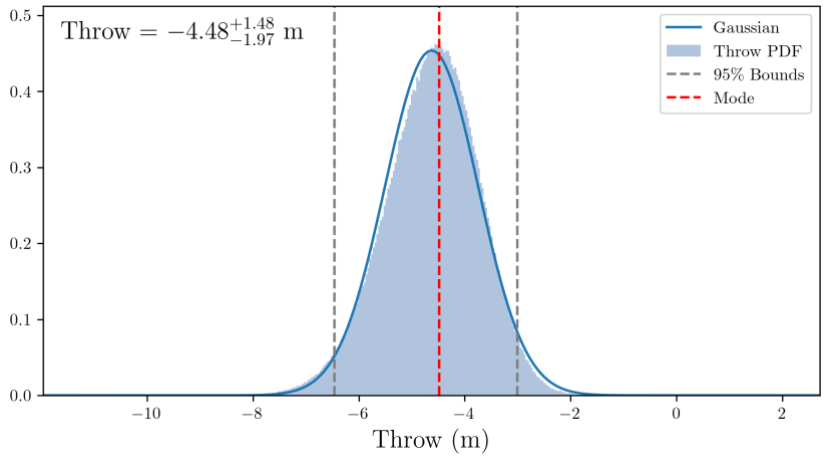

Profile 18

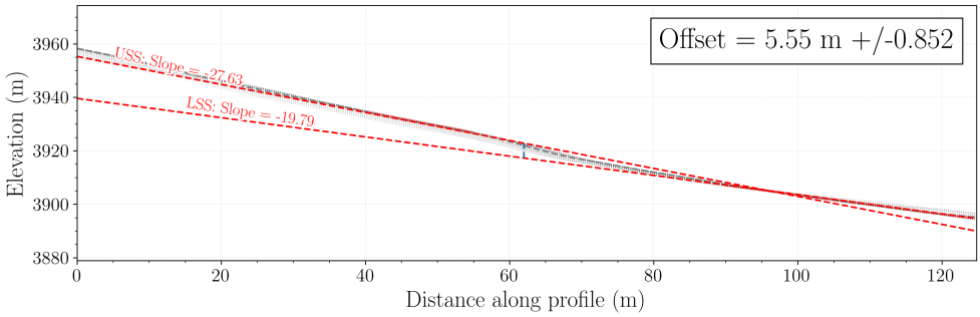

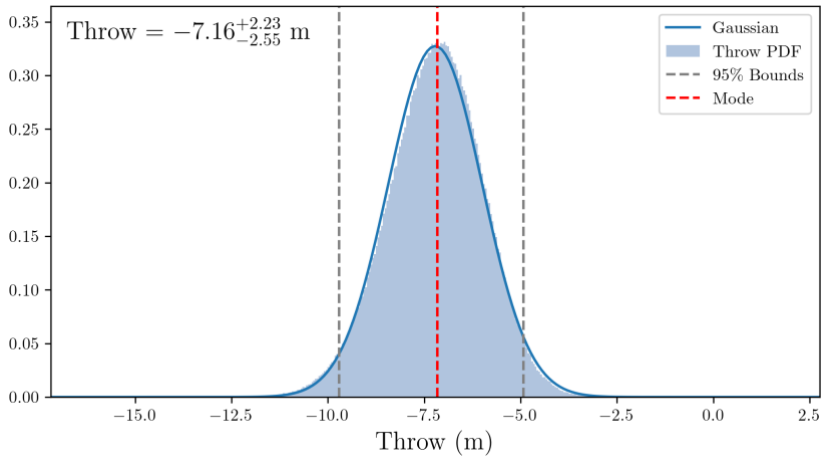

Profile 19

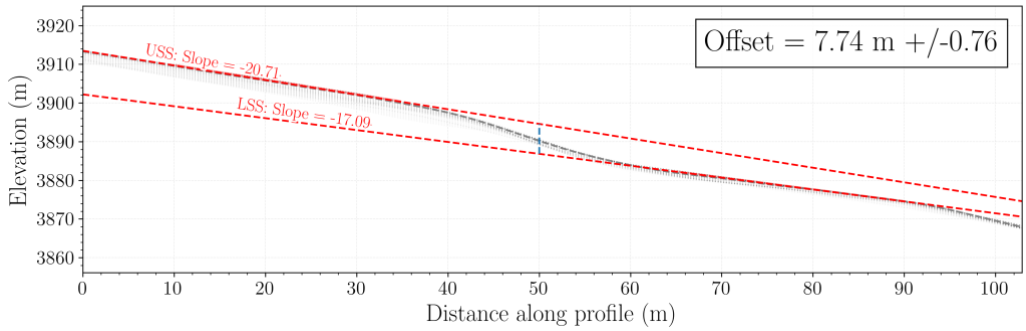

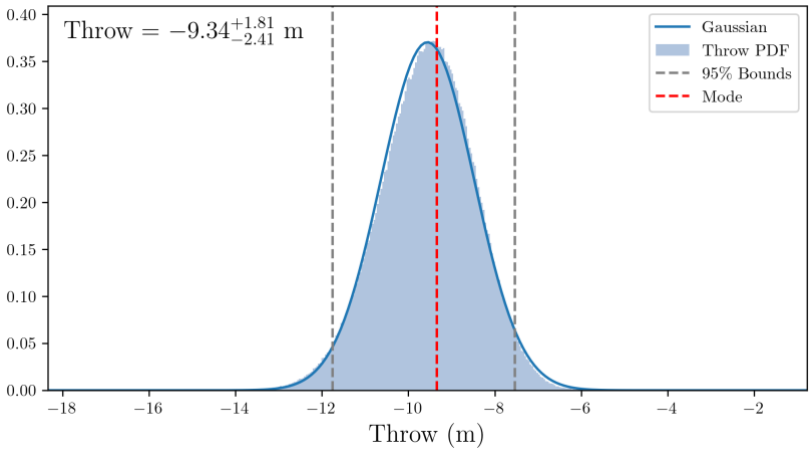

Profile 20

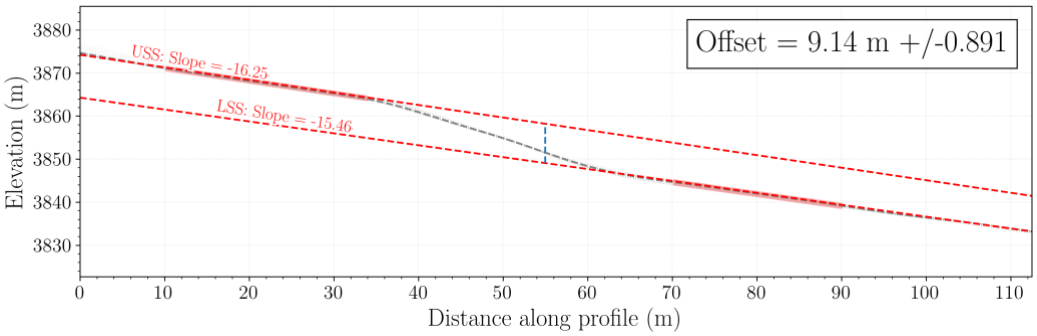

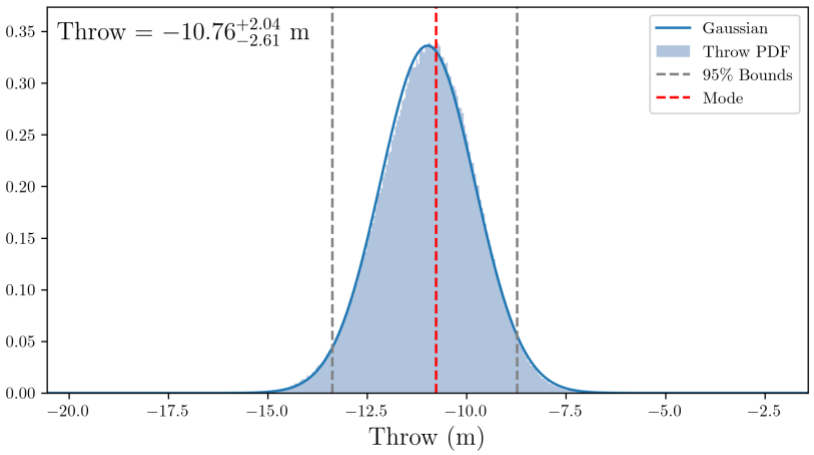

Profile 21

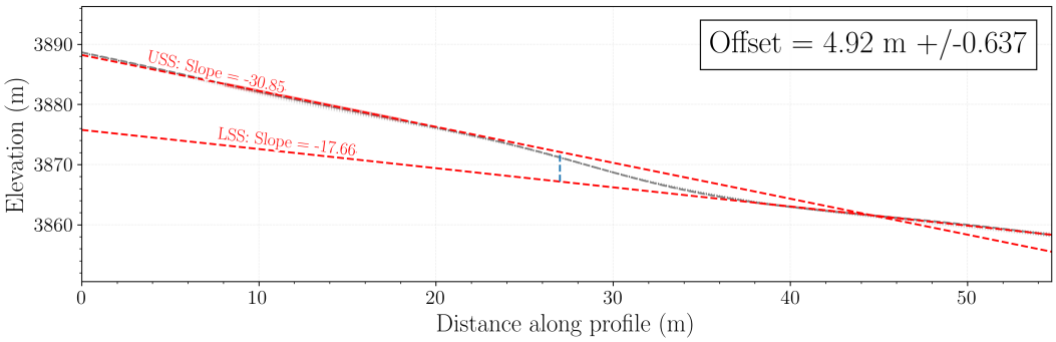
Offset = 4.92 m +/-0.637
USS: Slope = -30.85
LSS: Slope = -17.66
Elevation (m)
Distance along profile (m)

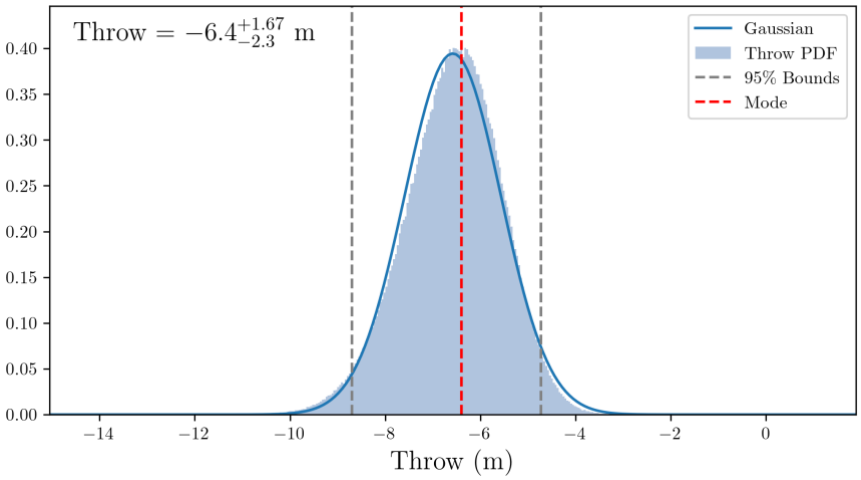
Throw = $-6.4^{+1.67}_{-2.3}$ m
Gaussian
Throw PDF
95% Bounds
Mode
Throw (m)

Figure SI-3: Plot generated using P-CAAT (Dortch et al., 2022) based on dataset from the eastern moraine (samples T1 to T7) and using the Std/IQR bandwidth estimator (bandwidth = 0.3482 ka; r-sq = 0.9986). The sample T4 (13.0 ± 0.5 ka) is detected as outlier (in grey). The six remaining samples form a single gaussian distribution (in red) with a peak at 14.51 ± 0.58 ka.

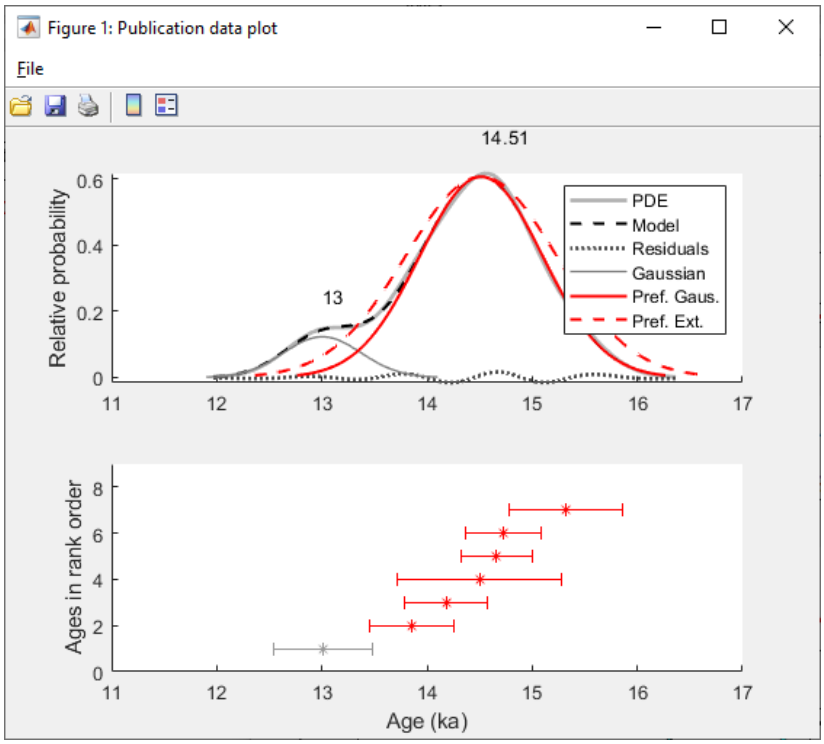

Figure SI-4: Plot generated using P-CAAT (Dortch et al., 2022) based on dataset from the western moraine (samples T8 to T11) and using the Std/IQR bandwidth estimator (bandwidth = 0.4453 ka; r-sq = 1.0000). Two samples (T3 = 15.3 ± 0.5 and T11 = 15.6 ± 0.5 ka) are detected as outliers (in grey). The three remaining samples form a single gaussian distribution (in red) with a peak at 14.15 ± 0.47 ka

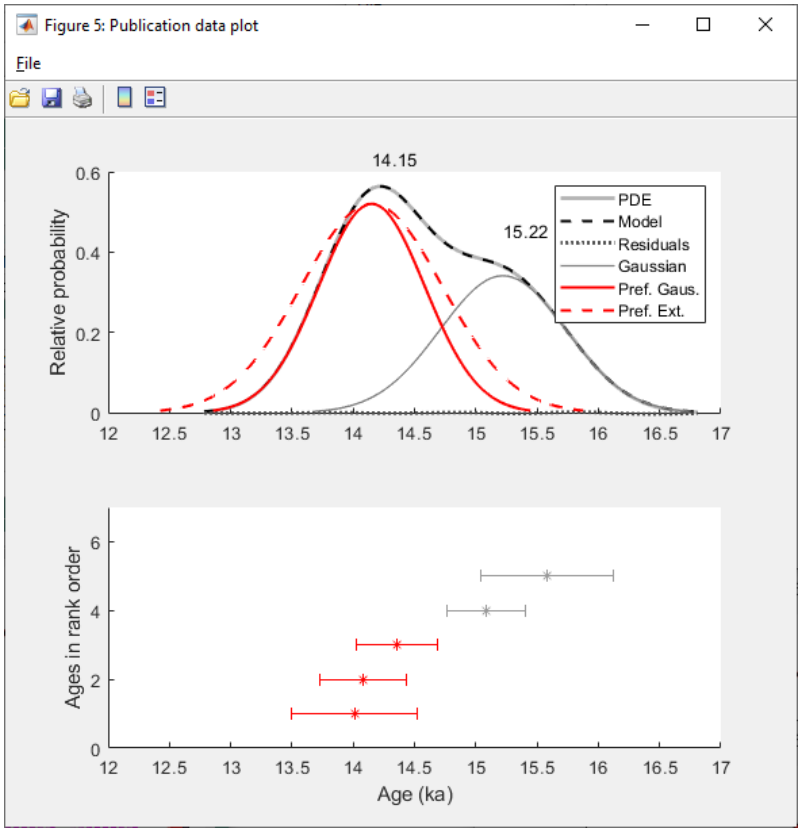

Figure SI-5. Location of DEMs used in the study.

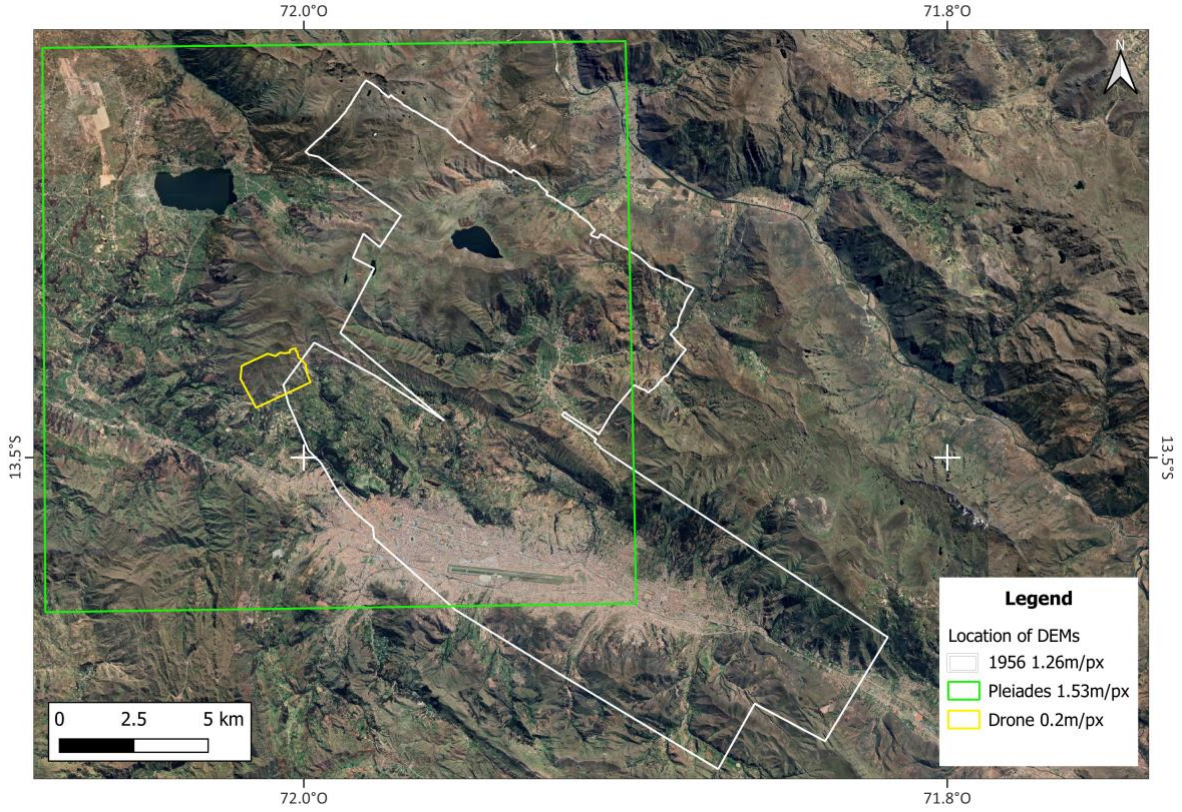

Figure SI-6. Trench ortomosaic, view to the east.

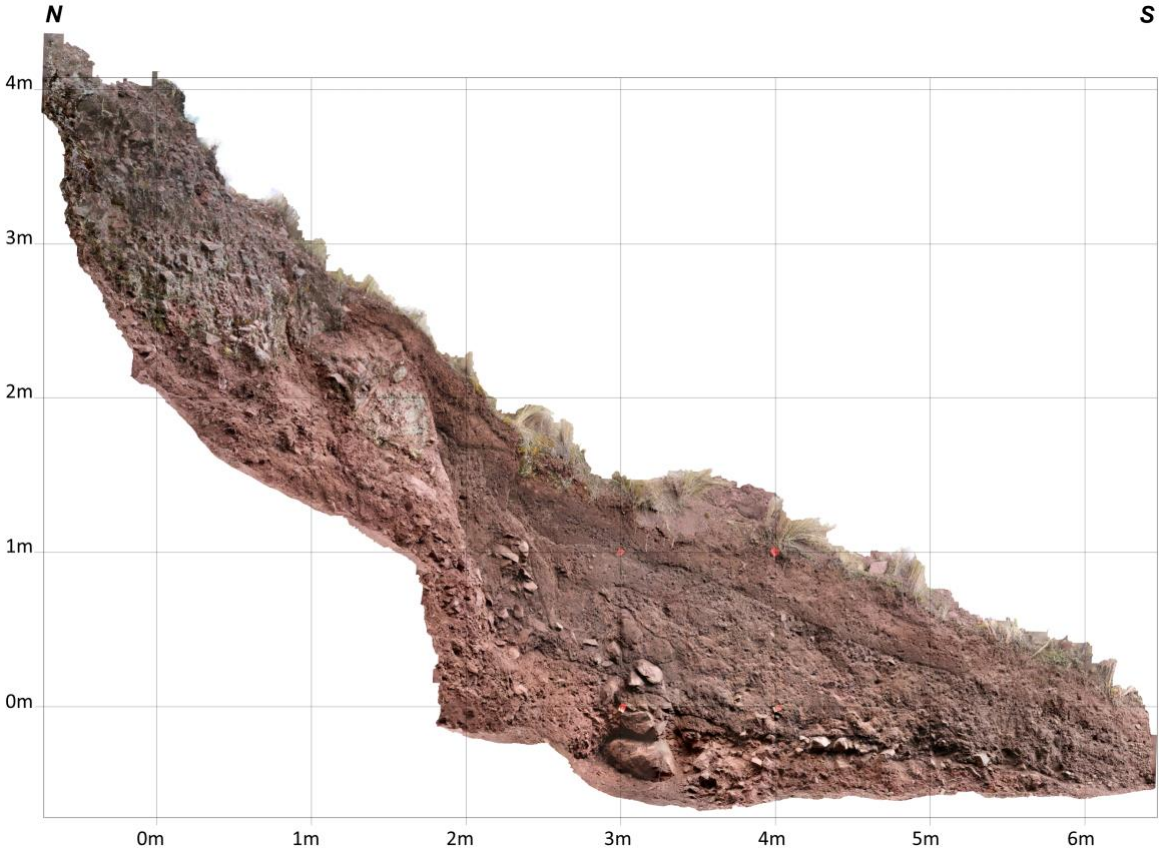

Photo SI-1: Slikenlines in the Tambomachay fault plane, located in the coordinates: latitude: -13.500648°; longitude: -71.924524°